Hadron Structure with DWF (II)

George T. Fleming

Yale University

3rd International Lattice Field Theory Network Workshop
Jefferson Lab, Newport News, VA

LHPC Hadron Structure project on USQCD resources

Dru Renner
University of Arizona
Ronald Babich, Richard Brower, James Osborn
Boston University
Rebecca Irwin, Michael Ramsey-Musolf
California Institute of Technology
Robert Edwards, Kostas Orginos (W&M), David Richards
Thomas Jefferson National Accelerator Facility
Bojan Bistrović, Jonathan Bratt, Patrick Dreher, Oliver Jahn,
John Negele, Andrew Pochinsky, Dmitry Sigaev
Massachusetts Institute of Technology
Matthias Burkardt, Michael Engelhardt
New Mexico State University
George Fleming
Yale University

LHPC – International Collaborators

Constantia Alexandrou, Antonios Tsapalis
University of Cyprus
Wolfram Schroers
NIC/DESY, Zeuthen
Philippe de Forcrand
ETH-Zürich and CERN
Philipp Hägler
Vrije Universiteit, Amsterdam

PDF's and Generalized PDF's (GPD's)

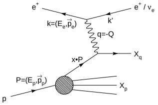

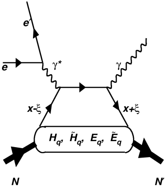

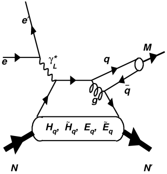

- Thanks to QCD factorization, very little knowledge of hadron structure needed for inclusive DIS reactions.
- A lot of information about hadron structure is lost in the inclusive sum over final states of remnant.
- Semi-inclusive and exclusive processes build two-dimensional pictures of hadrons (DVCS, DVMP, . . .)
- GPD's are PDF's with a transverse kick to struck parton before putting it back into the hadron.
  - More kinematic variables: $x = \frac{1}{2}(x_f + x_i)$, $\xi = \frac{1}{2}(x_f - x_i)$, t (or Q^2).
  - GPD's are **form factors** of the collection of partons with same **fixed** x.
  - As $\xi \to 0$ and $t \to 0$, GPD's must reduce to ordinary PDF's.
  - t dependence at **fixed** x should contain information about **spatial distribution** of all quarks with same x.

GPD's and Generalized Form Factors (GFF's)

- Experimentalists measure matrix elements of light cone operators

$$\left\langle P'S' \left| \mathcal{O}^q_\Gamma \right| PS \right\rangle = \left\langle P'S' \left| \overline{q}\left(-\frac{x^-}{2}\right) \Gamma \, \mathcal{P} \exp\left[-ig\int_{x^-/2}^{-x^-/2} A^+(y)dy\right] q\left(\frac{x}{2}\right) \right| PS \right\rangle$$

- They can be written in terms of GPD's [1]

$$\int \frac{dx^-}{2\pi} e^{ix^- \overline{p}^+ x} \left\langle P'S' \left| \mathcal{O}^q_\Gamma \right| PS \right\rangle = \overline{U}(P', S') \left[H^q(x,\xi,\Delta^2)\Gamma + E^q(x,\xi,\Delta^2) \frac{i\sigma\cdot\Delta}{2M} \right] U(P,S)$$

- Eight GPD's in all: H, E, $\widetilde{H}$, $\widetilde{E}$, H_T, E_T, $\widetilde{H}_T$, $\widetilde{E}_T$
- Using OPE, light cone operators replaced by tower of local twist two operators

$$\left\langle P'S' \left| \mathcal{O}^{\mu_1\cdots\mu_n}_\Gamma \right| PS \right\rangle = \left\langle P'S' \left| \overline{q}(x) iD^{(\mu_1} \cdots iD^{\mu_{n-1}} \Gamma^{\mu_n)} q(x) \right| PS \right\rangle$$

- They can be parameterized by generalized form factors (GFF's).

$$\left\langle P'S' \left| \mathcal{O}^{\mu_1\mu_2}_q \right| PS \right\rangle =$$

$$\overline{U}(P', S') \left[A^q_{20}(Q^2)\gamma^{(\mu_1}\Delta^{\mu_2)} + B^q_{20}(Q^2) \frac{i\sigma^{(\mu_1\alpha}\Delta^\alpha}{2M}\Delta^{\mu_2)} + C^q_2(Q^2)\frac{\Delta^{(\mu_1}\Delta^{\mu_2)}}{2M} \right] U(P,S)$$

- Nine GFF's: A_{ni}, B_{ni}, C_n, $\widetilde{A}_{ni}$, $\widetilde{B}_{ni}$, A_{Tni}, B_{Tni}, $\widetilde{A}_{Tni}$, $\widetilde{B}_{Tni}$

[1] X. D. Ji, hep-ph/9807358. Recent review: M. Diehl, Phys. Rept. **388**, 41-277 (2003).

Equivalence of GPD's and GFF's

- GPD's and GFF's are formally equivalent by Mellin transformation

$$\int_{-1}^{1} dx\, x^{n-1} H^q(x,\xi,Q^2) = \sum_{i=0,\ \mathrm{even}}^{n-1} A^q_{ni}(Q^2)(-2\xi)^i + \delta_{n,\ \mathrm{even}} C^q_n(Q^2)(-2\xi)^n$$
$$\int_{-1}^{1} dx\, x^{n-1} E^q(x,\xi,Q^2) = \sum_{i=0,\ \mathrm{even}}^{n-1} B^q_{ni}(Q^2)(-2\xi)^i - \delta_{n,\ \mathrm{even}} C^q_n(Q^2)(-2\xi)^n$$

- Choice of GPD's *vs.* GFF's depends on physics.

  GPD: PDF's and transverse PDF's
  GFF: elastic form factors and nucleon spin

- In Euclidean lattice QCD, only GFF's can be computed directly.
- Many GFF's are familiar experimental quantities:
  - $A^q_{10}(Q^2) = F^q_1(Q^2)$, $B^q_{10}(Q^2) = F^2_2(Q^2)$
  - $\widetilde{A}^q_{10}(Q^2) = G^q_A(Q^2)$, $\widetilde{B}^q_{10}(Q^2) = G^q_P(Q^2)$,
  - $J^q = \frac{1}{2}\left(A^q_{20}(0) + B^q_{20}(0)\right)$, $\frac{1}{2}\Delta\Sigma^q = \widetilde{A}^q_{10}(0)$
  - $L^q = J^q - \frac{1}{2}\Delta\Sigma^q$
  - $\left\langle x^{n-1}\right\rangle_q = A^q_{n0}(0)$, $\left\langle x^{n-1}\right\rangle_{\Delta q} = \widetilde{A}^q_{n0}(0)$, $\left\langle x^{n-1}\right\rangle_{\delta q} = A^q_{Tn0}(0)$

Summary of LHPC hadron structure program

- Long term program to compute all $n \leq 4$ GFF's in dynamical lattice QCD.
- Current pion masses $m_\pi \approx 300 - 750$ MeV and lattice spacing $a \approx \frac{1}{8}$ fm.
- Status of the calculation

Operators	Matrix elements	Operator renorm.	GFF extraction	Analysis
$\overline{q}\Gamma_{\mu} q$	Done!	Done!	Done!	Preliminary
$\overline{q}\Gamma_{(\mu} D_{\nu)} q$	Done!	Done!	Done!	Preliminary
$\overline{q}\Gamma_{(\mu} D_\nu D_{\rho)} q$	Done!	Done!	Done!	Very Preliminary
$\overline{q}\Gamma_{(\mu} D_\nu D_\rho D_{\sigma)} q$	Not yet	Done!	Not yet	Not yet

- Only isovector flavor combinations for GFF's in this round.
- Finite perturbative renormalization needed to quote results in $\overline{\mathrm{MS}}$ scheme.

$$\left\langle P'S' \left| \mathcal{O}_\Gamma^{\mu_1 \cdots \mu_n} \right| PS \right\rangle_{\overline{\mathrm{MS}}} = Z \left\langle P'S' \left| \mathcal{O}_\Gamma^{\mu_1 \cdots \mu_n} \right| PS \right\rangle_{\mathrm{latt}}$$

- Lighter pion masses $m_\pi \approx 250$ MeV finished by next year.

Perturbative renormalization of twist two matrix elements

Tree level: $Z = 1$, One loop HYP corrections: $< 10\%$.

operator	$H(4)$	NOS	HYP	APE
$\bar{q}[\gamma_5]q$	$1_1^{\pm}$	0.68	0.971	1.07
$\bar{q}[\gamma_5]\gamma_\mu q$	$4_4^{\mp}$	0.765	0.964	0.99
$\bar{q}[\gamma_5]\sigma_{\mu\nu} q$	$6_1^{\mp}$	0.821	0.987	0.989
$\bar{q}[\gamma_5]\gamma_{\{\mu}D_{\nu\}} q$	$6_3^{\pm}$	0.986	0.968	0.929
$\bar{q}[\gamma_5]\gamma_{\{\mu}D_{\nu\}} q$	$3_1^{\pm}$	0.972	0.962	0.925
$\bar{q}[\gamma_5]\gamma_{\{\mu}D_\nu D_{\alpha\}} q$	$8_1^{\mp}$	1.206	0.982	0.898
$\bar{q}[\gamma_5]\gamma_{\{\mu}D_\nu D_{\alpha\}} q$	mixing	8.78×10^{-3}	2.88×10^{-3}	1.26×10^{-3}
$\bar{q}[\gamma_5]\gamma_{\{\mu}D_\nu D_{\alpha\}} q$	$4_2^{\mp}$	1.191	0.98	0.898
$\bar{q}[\gamma_5]\gamma_{\{\mu}D_\nu D_\alpha D_{\beta\}} q$	$2_1^{\pm}$	1.375	0.989	0.876
$\bar{q}[\gamma_5]\sigma_{\mu\{\nu}D_{\alpha\}} q$	$8_1^{\pm}$	1.018	0.991	0.945
$\bar{q}[\gamma_5]\gamma_{[\mu}D_{\nu]} q$	$6_1^{\mp}$	0.967	0.973	0.983
$\bar{q}[\gamma_5]\gamma_{[\mu}D_{\{\nu]}D_{\alpha\}} q$	$8_1^{\pm}$	0.931	0.937	0.947

Table 11.17: Full $\overline{MS}$ to lattice renormalization coefficients for $M = 1.7$ and 1-loop expression for g. By chiral symmetry matrix elements are the same (except for parity) with and without γ_5, and this is indicated by the $[\gamma_5]$ notation where the upper parity arises in the absence of γ_5.

B. Bistrović, Ph. D. Thesis, MIT, 2005

Proton Electromagnetic Form Factors

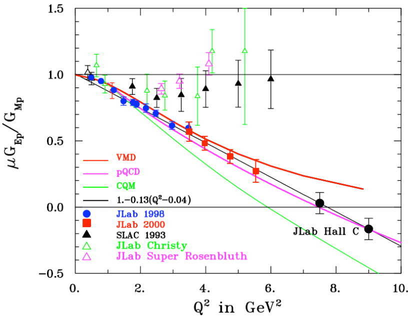

C. Perdrisat (W&M), JLab Users Group Meeting, June, 2005.

- Dramatic discrepancy between experimental techniques. Two photon exchange processes may be the cause.
- Data taking at $Q^2 = 9\ \mathrm{GeV}^2$ starting soon.
- Will Lattice QCD predict the vanishing of $G_E^p(Q^2)$ around $Q^2 = 8\ \mathrm{GeV}^2$?

Proton and Neutron Electromagnetic Form Factors

Empirical fit of experimental data

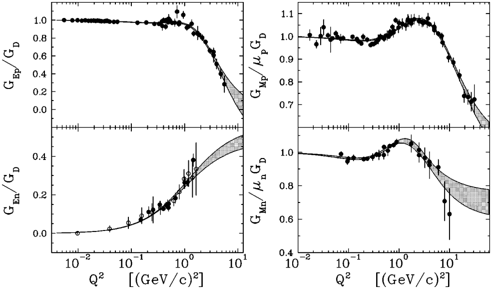

$$
\begin{aligned}
G(Q^2) &= \frac{G(0)}{1 + b_1\tau + b_2\tau^2} \\
\tau &= \frac{Q^2}{4m_p^2} \\
G_E^n(Q^2) &= \frac{A\tau}{1 + B\tau} G_D(Q^2) \\
G_D(Q^2) &= \frac{1}{(1 + Q^2/\Lambda^2)^2} \\
\Lambda^2 &= 0.71\ (\mathrm{GeV})^2
\end{aligned}
$$

J. J. Kelly (Maryland), Phys. Rev. C **70**, 068202 (2004)

- Using covariance matrix[2] these fits can be tranformed into Dirac-Pauli form with isospin decomposition.

[2] J. J. Kelly, private communication

Isospin decomposition of nucleon form factors

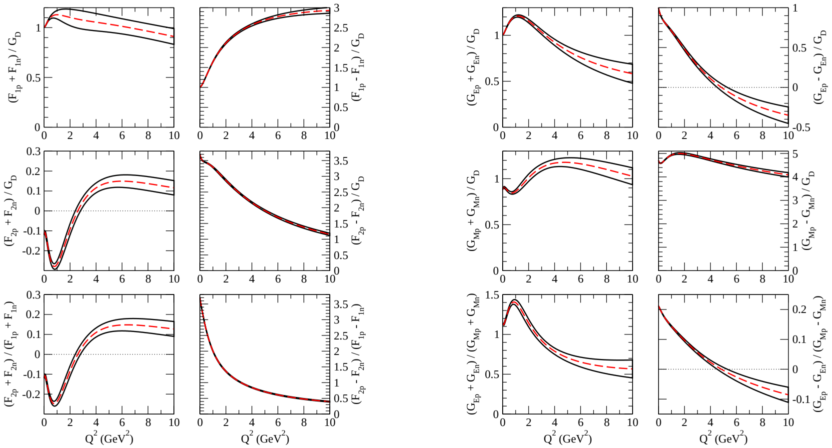

Nucleon Isovector F_1 (or A_{10}) Form Factor on the Lattice

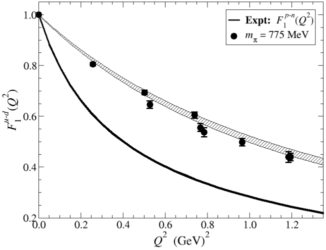

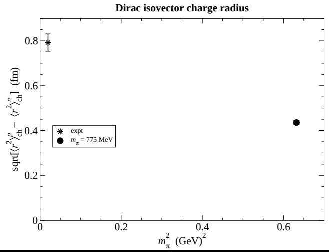

Preliminary

- For $Q^2 \lesssim 1\ \mathrm{GeV}^2$, fitting lattice data to dipole *ansatz* gives the Dirac charge radius $\langle r^2 \rangle_{\mathrm{ch}}^{u-d}$.
- Chiral extrapolation using leading analytic and non-analytic terms and finite range regulator (PRL **86** 5011).

$$\langle r^2 \rangle_{\mathrm{ch}}^{u-d} = a_0 - 2\frac{\left(1+5g_A^2\right)}{(4\pi f_\pi)^2}\frac{1}{2}\log\left(\frac{m_\pi^2}{m_\pi^2+\Lambda^2}\right)$$

- Best fit: $\Lambda \approx 740\ \mathrm{MeV}$.

Nucleon Isovector F_1 (or A_{10}) Form Factor on the Lattice

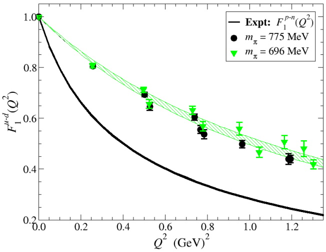

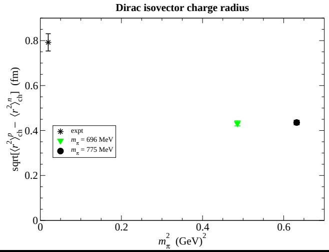

Preliminary

- For $Q^2 \lesssim 1\ \mathrm{GeV}^2$, fitting lattice data to dipole *ansatz* gives the Dirac charge radius $\left\langle r^2 \right\rangle_{\mathrm{ch}}^{u-d}$.
- Chiral extrapolation using leading analytic and non-analytic terms and finite range regulator (PRL **86** 5011).

$$\left\langle r^2 \right\rangle_{\mathrm{ch}}^{u-d} = a_0 - 2\frac{\left(1+5g_A^2\right)}{(4\pi f_\pi)^2}\frac{1}{2}\log\left(\frac{m_\pi^2}{m_\pi^2+\Lambda^2}\right)$$

- Best fit: $\Lambda \approx 740\ \mathrm{MeV}$.

Nucleon Isovector F_1 (or A_{10}) Form Factor on the Lattice

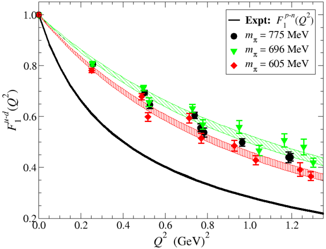

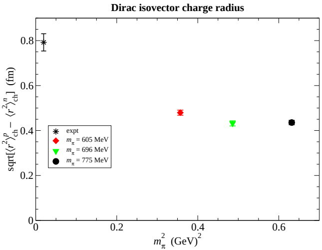

Preliminary

- For $Q^2 \lesssim 1\ \mathrm{GeV}^2$, fitting lattice data to dipole *ansatz* gives the Dirac charge radius $\langle r^2 \rangle^{u-d}_{\mathrm{ch}}$.
- Chiral extrapolation using leading analytic and non-analytic terms and finite range regulator (PRL **86** 5011).

$$\langle r^2 \rangle^{u-d}_{\mathrm{ch}} = a_0 - 2\frac{\left(1+5g_A^2\right)}{(4\pi f_\pi)^2}\frac{1}{2}\log\left(\frac{m_\pi^2}{m_\pi^2+\Lambda^2}\right)$$

- Best fit: $\Lambda \approx 740\ \mathrm{MeV}$.

Nucleon Isovector F_1 (or A_{10}) Form Factor on the Lattice

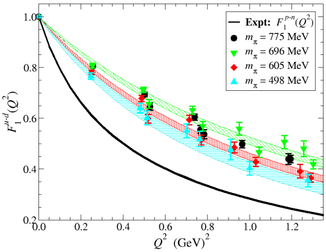

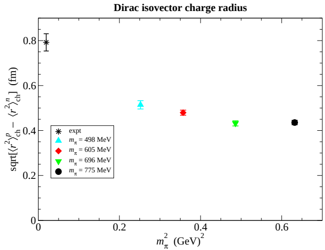

Preliminary

- For $Q^2 \lesssim 1\ \mathrm{GeV}^2$, fitting lattice data to dipole *ansatz* gives the Dirac charge radius $\langle r^2 \rangle_{\mathrm{ch}}^{u-d}$.
- Chiral extrapolation using leading analytic and non-analytic terms and finite range regulator (PRL **86** 5011).

$$\langle r^2 \rangle_{\mathrm{ch}}^{u-d} = a_0 - 2\frac{\left(1+5g_A^2\right)}{(4\pi f_\pi)^2}\frac{1}{2}\log\left(\frac{m_\pi^2}{m_\pi^2+\Lambda^2}\right)$$

- Best fit: $\Lambda \approx 740\ \mathrm{MeV}$.

Nucleon Isovector F_1 (or A_{10}) Form Factor on the Lattice

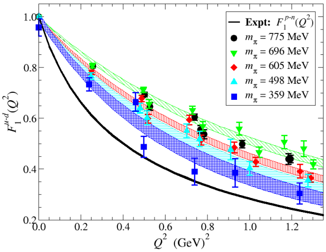

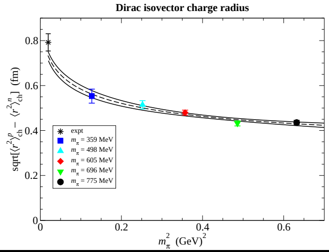

Preliminary

- For $Q^2 \lesssim 1$ GeV^2, fitting lattice data to dipole *ansatz* gives the Dirac charge radius $\langle r^2 \rangle_{\rm ch}^{u-d}$.
- Chiral extrapolation using leading analytic and non-analytic terms and finite range regulator (PRL **86** 5011).

$$\langle r^2 \rangle_{\rm ch}^{u-d} = a_0 - 2\frac{\left(1+5g_A^2\right)}{(4\pi f_\pi)^2}\frac{1}{2}\log\left(\frac{m_\pi^2}{m_\pi^2+\Lambda^2}\right)$$

- Best fit: $\Lambda \approx 740$ MeV.

Nucleon Isovector F_1 (or A_{10}) Form Factor on the Lattice

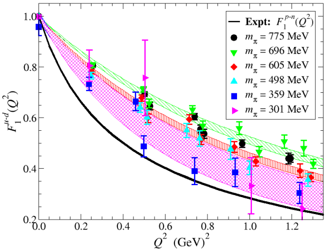

Dirac isovector charge radius

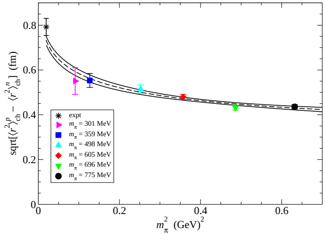

Preliminary

- For $Q^2 \lesssim 1\ \mathrm{GeV}^2$, fitting lattice data to dipole *ansatz* gives the Dirac charge radius $\left\langle r^2 \right\rangle_{\mathrm{ch}}^{u-d}$.
- Chiral extrapolation using leading analytic and non-analytic terms and finite range regulator (PRL **86** 5011).

$$\left\langle r^2 \right\rangle_{\mathrm{ch}}^{u-d} = a_0 - 2\frac{\left(1+5g_A^2\right)}{(4\pi f_\pi)^2}\frac{1}{2}\log\left(\frac{m_\pi^2}{m_\pi^2+\Lambda^2}\right)$$

- Best fit: $\Lambda \approx 740\ \mathrm{MeV}$.

Nucleon Isovector F_1 at Higher Q^2

Preliminary

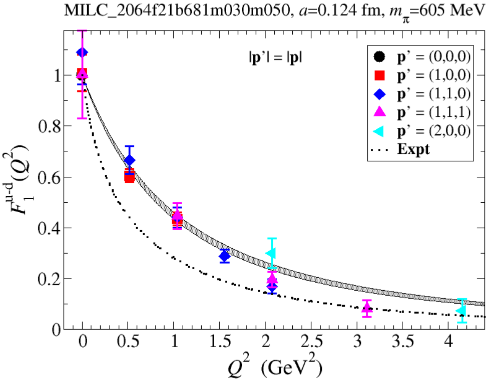

- Even at $m_\pi \approx 600$ MeV, extraction at higher Q^2 is noisy.
- Both polarization transfer experiments and lattice results still consistent with dipole *ansatz* up to 4 GeV^2.
- Lattice QCD simulations will need much more statistics to reach 8 GeV^2 before experiments.

Nucleon Isovector G_E at Higher Q^2

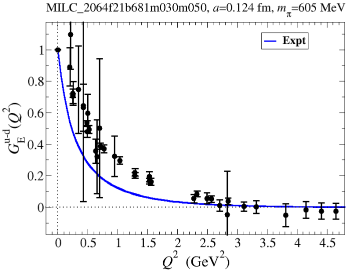

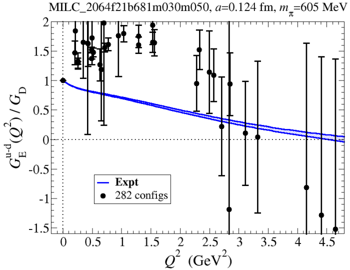

Preliminary

- Fits of experimental data suggest G_E^{u-d} vanishes around $Q^2 \sim 4\ \mathrm{GeV}^2$.
- With $m_\pi \approx 600\ \mathrm{MeV}$ on 282 configs, the lattice points are consistent with something interesting happening at $4\ \mathrm{GeV}^2$.
- Lattice QCD simulations will need more statistics to say anything more conclusive.

Nucleon Isovector Ratio F_2/F_1

Preliminary

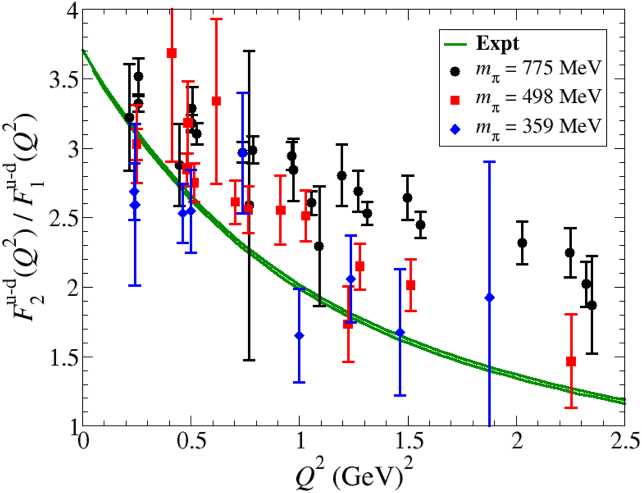

Axial Charge: $g_A = \langle 1 \rangle_{\Delta u - \Delta d} = \widetilde{A}_{10}^{u-d}(0)$

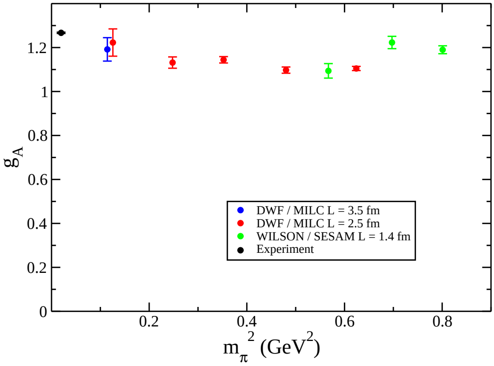

Dru B. Renner, Lattice 2005

Tensor Charge: $g_T = \langle 1 \rangle_{\delta u - \delta d} = A^{u-d}_{T10}(0)$

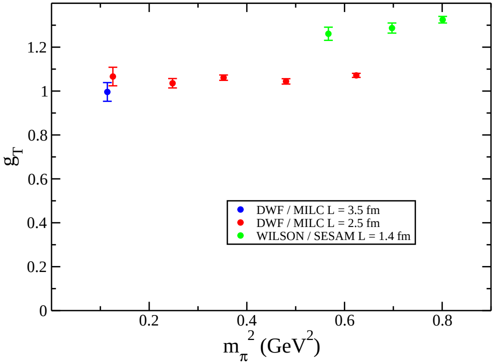

Dru B. Renner, Lattice 2005

Momentum Fraction: $\langle x \rangle_{u-d} = A_{20}^{u-d}(0)$

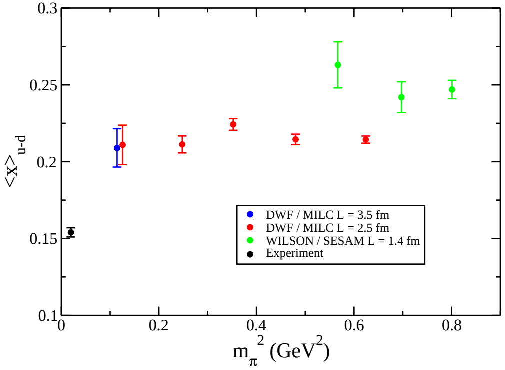

Dru B. Renner, Lattice 2005

Polarized Momentum Fraction: $\langle x \rangle_{\Delta u - \Delta d} = \widetilde{A}_{20}^{u-d}(0)$

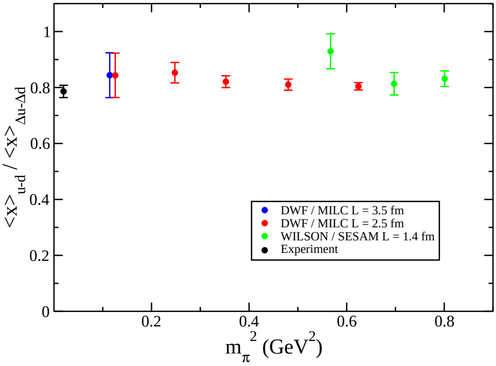

Dru B. Renner, Lattice 2005

Transverse quark distributions

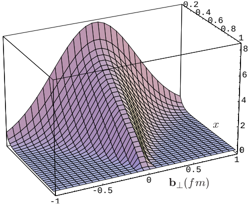

M. Burkardt hep-ph/0207047

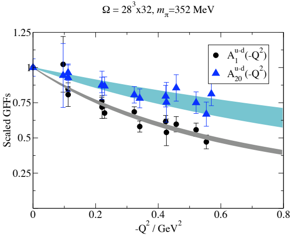

W. Schroers, Lattice 2005

$$A^q_{n0}(-\Delta^2_\perp) = \int d^2 b_\perp \, e^{i\mathbf{\Delta}_\perp \cdot \mathbf{b}_\perp} \int_{-1}^{1} x^{n-1} q(x, \mathbf{b}_\perp)$$

$$\left\langle b^2_\perp \right\rangle^q_{(n)} = -4 \frac{A^{q\prime}_{n0}(0)}{A^q_{n0}(0)}$$

$$\lim_{x \longrightarrow 1} q(x, \mathbf{b}_\perp) \propto \delta(b^2_\perp)$$

- Higher moments A_{n0} weight $x \sim 1$.
- Slope of A^q_{n0} decreases as n increases.

Summary and outlook

- Large scale computation of isovector matrix elements $(n \leq 3)$ is done. Data analysis is proceeding rapidly. Expect published results soon.
- Perturbative renormalization complete. B. Bistrović (MIT)
- Reaching higher Q^2 is high priority for nucleon form factors.
- Isoscalar and strange matrix elements are $\mathcal{O}(10) - \mathcal{O}(100)$ times harder to compute due to statistical noise. We're making our first serious attempt this year.